Journal of Power Sources 271 (2014) 342–345

Contents lists available at ScienceDirect

Journal of Power Sources

journal homepage: www.elsevier.com/locate/jpowsour

Short communication

A synthesis of crystalline $Li_7P_3S_{11}$ solid electrolyte from 1,2-dimethoxyethane solvent

Seitaro Ito [a, *], Moeka Nakakita [b], Yuichi Aihara [a], Takahiro Uehara [b], Nobuya Machida [b]

[a] Samsung R&D Institute Japan, Minoh Semba Center Bldg, 13F, Semba Nishi 2-1-11, Minoh, Osaka, 562-0036, Japan
[b] Department of Chemistry, Konan University, Okamoto 8-9-1, Higashinada-ku, Kobe, Hyogo, 658-8501, Japan

HIGHLIGHTS

- A $Li_7P_3S_{11}$ crystal was synthesized from a liquid phase for the first time.
- Ionic conductivity of 2.7×10^{-4} S cm^{-1} at 25 °C was obtained in $Li_7P_3S_{11}$.
- At the production aspect, the liquid method is one of promising synthesis.

ARTICLE INFO

Article history:
Received 1 April 2014
Received in revised form
29 July 2014
Accepted 5 August 2014
Available online 14 August 2014

Keywords:
Sulfide
Ion conductor
Liquid phase synthesis
Solid electrolyte
Solid state battery

ABSTRACT

A crystalline solid electrolyte, $Li_7P_3S_{11}$, was synthesized by a liquid-phase reaction of Li_2S and P_2S_5 in an organic solvent. A precursor, which was a mixture of solvated Li_3PS_4 and $Li_4P_2S_7$, was prepared by mixing Li_2S and P_2S_5 powders in 1,2-dimethoxyethane (DME) solvent. After a vacuum drying of the precursor, the crystalline phase of $Li_7P_3S_{11}$ was obtained by heat treatment at 250 °C for 1 h in Ar atmosphere. The $Li_7P_3S_{11}$ sample showed high ionic conductivity of 2.7×10^{-4} S cm^{-1} at room temperature. The liquid-phase synthesis of the solid electrolyte has advantages for mass-production of all-solid-state batteries.

1. Introduction

All-solid-state lithium ion batteries have received remarked attention because of their high safety. One of the key components of the solid-state batteries is the solid electrolytes, and extensive studies have been conducted on the promising materials including NASICON [1–4], garnet [5], and some sulfides [6]. It is well known that some of the materials show high ionic conductivity comparable to liquid state electrolytes [7,8]. However, there are only a few reports on the application of practical level of all-solid-state batteries [9]. The main reason is that the effective formation of solid–solid interface between the solid electrolytes and electrode active materials is rather challenging. For example, an oxide type solid electrolyte generally shows a large grain boundary resistance [10–12]. NASICON type solid electrolyte is also not appropriate since it is unstable against lithium metal because of its irreversible reactivity [13,14]. On the other hand, some sulfide-based solid electrolytes are particularly promising, since they show high ionic conductivity without any grain boundary resistance [15,16].

The solid sulfide electrolytes are generally synthesized from the mixture of Li_2S and P_2S_5 powder by high-energy ball milling process [17]. Furthermore, an ionic conductivity increased with the precipitation of high-ion-conductive crystalline phase by heat treatment [18,19]. However, it is difficult to scale up the production by high-energy ball-milling and/or melt-quenching method because these processes need high synthesis energy. Recently, a new method by using an organic solvent has been reported for synthesizing Li_3PS_4. This synthesis has been carried out under the existence of tetrahydrofuran (THF) [20] or hydrazine [21] as the solvent. This solid electrolyte showed high ionic conductivity more than 10^{-4} S cm^{-1}. The liquid phase synthesis method can be particularly efficacious for the large scale production and reduction of the energy cost compared to the conventional synthesis methods. However, the suitable solvent and synthesis condition have not been clear in liquid phase synthesis yet.

* Corresponding author. Tel.: +81 72 830 2962; fax: +81 72 730 2954.
E-mail addresses: sito@samsung.com, 34sito34@gmail.com (S. Ito).

http://dx.doi.org/10.1016/j.jpowsour.2014.08.024
0378-7753/

In this paper, we report the synthesis of a crystalline $Li_7P_3S_{11}$ by liquid phase reaction using 1,2-dimethoxyethane (DME) solvent. THF (cyclic ether structure) was reported as a solvent for the synthesis of Li_3PS_4 [20]. However, THF is a low-boiling-point solvent (b.p. 66 °C), and a high-boiling-point solvent is more suitable for industry applications. Furthermore, di-ether structure has an advantage in order to coordinate with lithium ion than mono-ether structure like THF. As mentioned above, we selected DME as a synthesis solvent because DME has a simple structure with two ether groups in the molecule, and its boiling-point (b.p. 83 °C) is higher than that of THF (b.p. 66 °C). Generally, $Li_7P_3S_{11}$ is made from 70 mol % of Li_2S and 30 mol% of P_2S_5 mixture by using of two step preparation process. The first step is the high-energy ball-milling process, which gives an amorphous precursor. The second step is heat treatment of the precursor and gives crystalline $Li_7P_3S_{11}$ phase. We prepared the $Li_7P_3S_{11}$ from 70 mol% of Li_2S and 30 mol% of P_2S_5 in DME solvent, and investigated the crystal structure and ionic conductivity of the obtained material. Two types of sulfide-anion structural units PS_4^{3-} and $P_2S_7^{4-}$ were observed in the obtained samples and the crystal structure of the obtained sample corresponds to the structure of well-known $Li_7P_3S_{11}$ crystal. The ionic conductivity of the obtained crystalline sample was 2.7×10^{-4} S cm^{-1} at 25 °C, which was one digit lower than that of the $Li_7P_3S_{11}$ crystal given in the ordinary two-step synthesis method.

2. Experimental

The $Li_7P_3S_{11}$ sulfide solid electrolyte was synthesized from Li_2S (Aldrich 99%) and P_2S_5 (Aldrich 99%) powders. 1,2-Dimethoxyethane (DME, Kishida chemical, LB grade) was used as a solvent. 0.488 g of Li_2S and 1.012 g of P_2S_5 were stirred for 3 days in 40 mL of the organic solvent at room temperature. The weight ratio of 0.488 g/1.012 g of Li_2S/P_2S_5, equivalent to the molar ratio of 70/30, was used in the synthesis. After the reaction, the organic solvent was removed by using a rotary evaporator. White powder was obtained and then dried under vacuum condition at 180 °C. After drying, the powder was heated at 200, 250 and 300 °C in Ar atmosphere in order to crystallize into the $Li_7P_3S_{11}$ phase. Generally, the $Li_7P_3S_{11}$ crystallization peak in DSC was observed above 300 °C in the case of the sulfide powder synthesized by ball milling method. However, the $Li_7P_3S_{11}$ crystallization peak around 200 °C was observed in DSC measurement in the case of the sulfide powder synthesized by the liquid-phase synthesis method (Fig. S1 in supplemental information). Therefore, the heat treatment temperature was set between 200 and 300 °C. All the above processes were carried out under Ar atmosphere because the sulfide electrolyte easily reacts with moisture in the air.

Powder X-ray diffraction (XRD) pattern was measured using a Multiflex XRD system (CuKα, 40 kV, 40 mA, Rigaku, Tokyo) for verifying the crystal structure. Raman spectroscopy was done using NRS-3100 (JASCO, Tokyo) in order to verify the phosphorus-sulfide anion structure in the obtained samples.

The ionic conductivities of the samples were determined by ac impedance measurements. In advance to the impedance measurement, the samples were pelletized into disks of 10 mm in diameter by a hydraulic press at 380 MPa. Indium foils were used for the blocking electrodes and attached to the both side of the pellets. The ac impedance measurements were performed within a frequency range of 2×10^6 Hz–20 Hz under an argon flow using a precision LCR meter (Agilent, E4980A).

3. Result and discussion

Li_2S powder partially dissolved in DME and the color of the liquid phase changed from colorless to light blue. On the other hand, P_2S_5 powder did not dissolve in DME. Although Li_2S and P_2S_5 powder were homogeneously dispersed in DME, a white precipitate immediately appeared after the mixing of those dispersion liquids. During the reaction, the color of the solution changed from greenish yellow to light bluish green. Finally, the colorless solution and the white precipitate were obtained. Thus, we thought that the chemical reaction occurred in the liquid phase. However, the reaction product (the precursor for the $Li_7P_3S_{11}$ preparation) was dispersed as white powders in DME (as a suspension). Raman spectra of the clear supernatant liquid showed that there were no PS_4^{3-} and $P_2S_7^{4-}$ anions in the clear supernatant liquid (Fig. S2 in supplemental information). This result indicates that PS_4^{3-} and $P_2S_7^{4-}$ anions are all in the precipitation.

Once the samples were prepared, we examined their crystal structures by powder XRD. Fig. 1 shows the powder XRD pattern of sulfide samples synthesized by DME solvent (a) before vacuum drying at 180 °C, (b) before and after heat treatment at (c) 200 °C, (d) 250 °C and (e) 300 °C. The alternating ordered structure of the PS_4^{3-} and $P_2S_7^{4-}$ units was reported for the case of $Li_7P_3S_{11}$ crystal synthesized by ball milling method [19]. Before vacuum drying sample at 180 °C (Fig. 1(a)), some XRD patterns were observed because of the complex formation with DME. The sulfide sample before heat treatment (after vacuum drying at 180 °C) showed an amorphous structure. Amorphous MoS_3 can be obtained by thermal decomposition of an ammonium thio-molybdate salt, $(NH_4)_2MoS_4$. In the amorphous MoS_3 preparation, some gases, such as NH_3 and H_2S, generate during the thermal decomposition. The generation of the gases distorts the crystal structure and makes it in amorphous state [22]. We presume that the similar phenomenon occurred in the sulfide solvated by DME. For the sulfide samples after 200 °C and 250 °C heat treatment, all the diffraction peaks corresponded well to the $Li_7P_3S_{11}$ mode by the ball milling method. Although excess heat treatment makes transition from $Li_4P_2S_7$ into $Li_4P_2S_6$, which is more stable and lower ionic conducting phase than $Li_4P_2S_7$, any peaks originated in $Li_4P_2S_6$ structure was not found in the sulfide samples after 200 °C and 250 °C heat treatment. On the other hand, $Li_4P_2S_6$ structure appeared in the sample heat-treated at 300 °C. These results indicate that the heat treatment condition between 200 °C and 250 °C was adequate and the $Li_7P_3S_{11}$ obtained by the liquid-phase methods gave the same crystal structure with that of the ball-milling process. It should be noted that some amorphous phase still remained in the sample

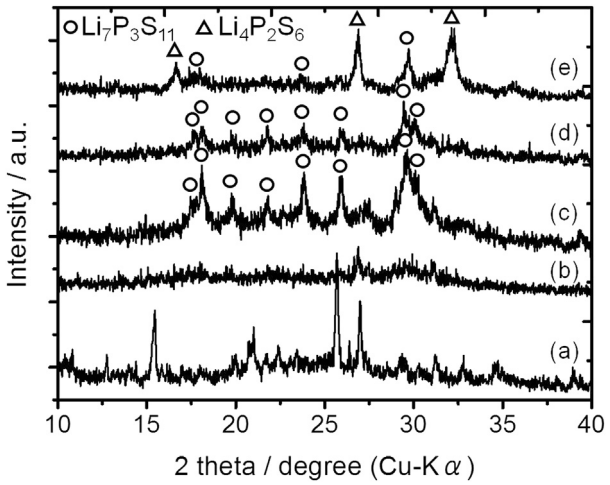

Fig. 1. The XRD patterns of the sulfide powder samples using DME solvent. The drying and heating conditions are: (a) before vacuum drying, (b) before heat treatment, and after heat treatment at (c) 200 °C, (d) 250 °C, and (e) 300 °C.

according to the broad XRD pattern, but it is unclear what fraction of the sample was actually crystallized merely from the XRD pattern.

Coordination of the chemical species in the samples was further characterized by the Raman spectra. The spectra of the sulfide samples synthesized by DME solvent (a) before vacuum drying, (b) before heat treatments and after (c) 200 °C, (d) 250 °C and (e) 300 °C of heat treatment are given in Fig. 2. The crystalline $Li_7P_3S_{11}$ synthesized by the ball-milling process and/or the melt-quenching methods is consisted of stoichiometric proportion 1:1 of Li_3PS_4 and $Li_4P_2S_7$ sulfide [19]. According to the literature, the Raman shifts of 420 cm^{-1} and 405 cm^{-1} are attributed to the PS_4^{3-} and $P_2S_7^{4-}$ anions, respectively [18]. The PS_4^{3-} and the $P_2S_7^{4-}$ anion peaks were found in the sulfide powder given by the liquid method in Fig. 2(b)–(d). During the heat treatment, the PS_4^{3-} anion did not shift from 420 cm^{-1}. On the other hand, the $P_2S_7^{4-}$ anion shifted from 391 cm^{-1} to 405 cm^{-1} (Fig. 2(a)). This probably indicates that the solvent, DME, interacted with $P_2S_7^{4-}$ anion because the distance between $P_2S_7^{4-}$ anion and Li^+ counter ion was changed by DME solvation, and the PS_4^{3-} anion was not influenced. Therefore, the Raman shift of 391 cm^{-1} was presumed to be the DME solvated $P_2S_7^{4-}$ structure unit and DME solvent perfectly removed from the sample by the heat treatments above 200 °C. This peak shift of the $P_2S_7^{4-}$ structure unit was observed in a sulfide sample synthesized by 1,2-diethoxyethane (DEE) solvent case, but not in a sample synthesized by the THF solvent. This result indicates that the solvated $P_2S_7^{4-}$ structure unit with THF (cyclic ether) is different from that with DME and/or DEE (linear ether). After 300 °C heat treatment, the $P_2S_7^{4-}$ peak shifted from 405 cm^{-1} to 386 cm^{-1}, which is attributed to $P_2S_6^{4-}$ unit. This result agrees well with the XRD observation. Although the detail reaction process is unclear, DME is suitable for the $Li_7P_3S_{11}$ (Li_3PS_4 and $Li_4P_2S_7$ mixture) synthesis, because one of byproducts, $Li_4P_2S_6$ was not observed in Raman measurement below 250 °C heat treatment.

Fig. 3 shows the temperature dependence of the conductivity for the sulfide samples synthesized by DME before and after 200 °C, 250 °C and 300 °C heat treatments. The ionic conductivity increased by the heat treatment for the $Li_7P_3S_{11}$ crystallization. The conductivity of 2.7×10^{-4} S cm^{-1} of the crystalline sample was confirmed at 298 K. On the contrary, 4.1×10^{-3} S cm^{-1} has been reported for the crystallized $Li_7P_3S_{11}$ prepared by use of the conventional ball-milling process [19]. The ionic conductivity of $Li_7P_3S_{11}$ obtained by the liquid-phase method is around 1/10 compared to the solid method.

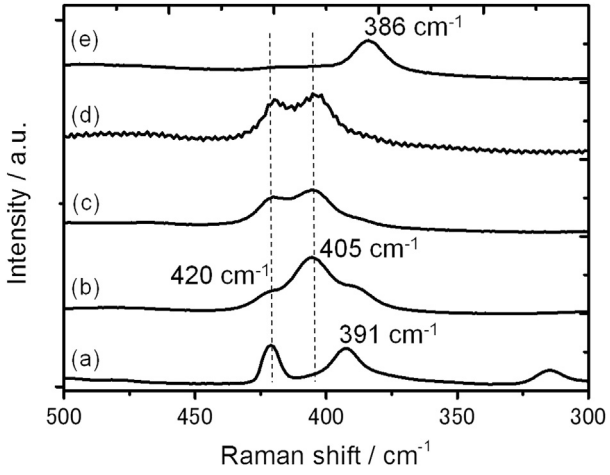

Fig. 2. The Raman spectra of the sulfide powders using DME solvent. The drying and heating conditions are: (a) before vacuum drying, (b) before heat treatment, and after heat treatment at (c) 200 °C, (d) 250 °C, and (e) 300 °C.

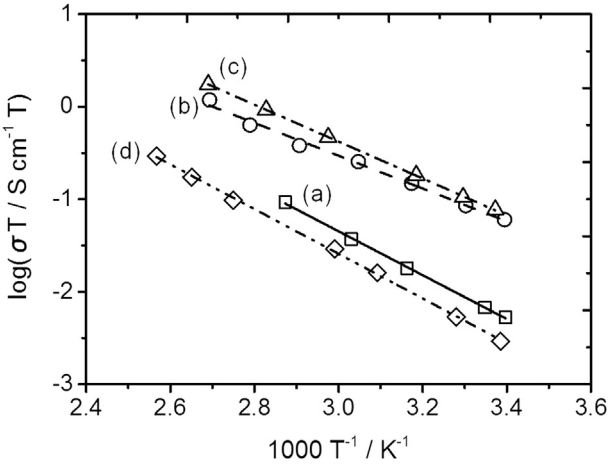

Fig. 3. The temperature dependence of the ionic conductivities for the sulfide powder before (a) and after 200 °C (b), 250 °C (c), and 300 °C (d) of heat treatment.

The reason for the discrepancy is that the crystallinity of the sample was still low as the XRD pattern indicated. Further optimization of heat treatment condition is needed in order to attain high crystallinity of $Li_7P_3S_{11}$. The ionic conductivity of the 300 °C-heat-treated sulfide sample was found to be 1.2×10^{-5} S cm^{-1} at 298 K; significantly lower than that of the 250 °C heat-treated sample. This is because of the $Li_4P_2S_7$ transition into $Li_4P_2S_6$ phase as seen in the XRD and Raman spectra. From the SEM image of the 250 °C heat treated sulfide sample, the particle size was 5–10 μm (Fig. S3 in supplemental information). This particle size does not differ vastly from that of the sample made by ball-milling method. The activation energy of the ionic conductivity of the 250 °C-heat-treated sample was 38 kJ mol^{-1}. This value is two times higher than that of the conventional ball-milled $Li_7P_3S_{11}$ [19]. It was presumed that the impurities from the solvent or partially remained amorphous phase in the sample increased the activation energy. We presume that the impurity phase or the amorphous phase precipitated at the interface among $Li_7P_3S_{11}$ crystal particles. Those impurity or amorphous phases form at the grain boundaries of the pellets for the ion-conductivity measurements. Lithium ions have to pass through those grain boundaries with low ion-conductivity. Therefore, the ionic conductivity and the activation energy of the pellet depend strongly on those phases. This is the reason of the low ionic conductivity and high activation energy.

4. Conclusion

We have successfully synthesized a crystal phase of $Li_7P_3S_{11}$ sulfide solid electrolyte by the liquid phase synthesis method. The processing energy and reaction time were significantly reduced in comparison with the conventional solid phase reaction. The synthesized $Li_7P_3S_{11}$ solid electrolyte showed the same crystal structure as that of the solid phase reaction. The ionic conductivity of 2.7×10^{-4} S cm^{-1} was verified at 298 K. The ionic conductivity of the $Li_7P_3S_{11}$ given by the liquid method is one digit lower than that given in the solid phase synthesis method. Considering a large scale production, the liquid state synthesis is probably one of the promising synthesis methods. Further, improvement of the crystallinity and purity of the product is required to achieve high ionic conductivity.

Appendix A. Supplementary data

Supplementary data related to this article can be found at http://dx.doi.org/10.1016/j.jpowsour.2014.08.024.

References

[1] J.B. Goodenough, H.Y.P. Hong, J.A. Kafalas, Mater. Res. Bull. 11 (1976) 203–220.
[2] H.Y.P. Hong, Mater. Res. Bull. 13 (1979) 117–124.
[3] M.A. Subramanian, R. Subramanian, A. Clearfield, Solid State Ionics 18&19 (1986) 562–569.
[4] H. Aono, E. Sugimoto, Y. Sadaoka, N. Inanaka, G. Adachi, J. Electrochem. Soc. 156 (1989) 590–591.
[5] R. Murugan, V. Thangadurai, W. Weppner, Angew. Chem. Int. Ed. 46 (2007) 7778–7781.
[6] M. Tatsumisago, F. Mizuno, A. Hayashi, J. Power Sources 159 (2006) 193–199.
[7] F. Mizuno, A. Hayashi, K. Tadanaga, M. Tatsumisago, Adv. Mater. 17 (2005) 918–921.
[8] N. Kamaya, K. Homma, Y. Yamakawa, M. Hirayama, R. Kanno, M. Yonemura, T. Kamiyama, Y. Kato, S. Hama, K. Kawamoto, A. Mitsui, Nat. Mater. 10 (2011) 682–686.
[9] S. Ito, S. Fujiki, T. Yamada, Y. Aihara, Y. Park, T.Y. Kim, S.W. Baek, J.M. Lee, S. Doo, N. Machida, J. Power Sources 248 (2014) 943–950.
[10] C.R. Mariappan, M. Gellert, C. Yada, F. Rosciano, B. Roling, Electrochem. Commun. 14 (2012) 25–28.
[11] H. Aono, E. Sugimoto, Y. Sadaoka, N. Imanaka, G. Adachi, Chem. Lett. (1990) 331–334.
[12] H. Aono, E. Sugimoto, Y. Sadaoka, N. Imanaka, G. Adachi, J. Electrochem. Soc. 137 (1990) 1023–1027.
[13] N. Imanishi, S. Hasegawa, T. Zhang, A. Hirano, Y. Takeda, O. Yamamoto, J. Power Sources 185 (2008) 1392–1397.
[14] K. Nagata, T. Nanno, J. Power Sources 174 (2007) 832–838.
[15] M. Tatsumisago, S. Hama, A. Hayashi, H. Morimoto, T. Minami, Solid State Ionics 154–155 (2002) 635–640.
[16] K. Hayamizu, Y. Aihara, Solid State Ionics 238 (2013) 7–14.
[17] A. Hayashi, S. Hama, H. Morimoto, M. Tatsumisago, T. Minami, J. Am. Ceram. Soc. 84 (2001) 477–479.
[18] F. Mizuno, A. Hayashi, K. Tadanaga, M. Tatumisago, Adv. Mater. 17 (2005) 134–137.
[19] K. Minami, A. Hayashi, M. Tatsumisago, J. Ceram. Soc. Jpn. 118 (4) (2010) 305–308.
[20] Z. Liu, W. Fu, E.A. Payzant, X. Yu, Z. Wu, N.J. Dudney, J. Kiggans, K. Hong, A.J. Rondidone, C. Liang, J. Am. Chem. Soc. 135 (2013) 975–978.
[21] Y. Wang, Z. Liu, X. Zhu, Y. Tang, F. Huang, J. Power Sources 224 (2013) 225–229.
[22] Th Weber, J.C. Muijsers, J.W. Niemantsverdriet, J. Phys. Chem. 99 (1995) 9194–9200.